Highly selective immobilization of amoxicillin antibiotic on carbon nanotube modified electrodes and its antibacterial activity†

Annamalai Senthil Kumar,*[a] Sundaram Sornambikai,[a] Lakshmipathy Deepika[b] and Jyh-Myng Zen[c]

Received 13th July 2010, Accepted 17th August 2010
DOI: 10.1039/c0jm02262d

An electrochemical route for highly selective immobilization of a β-lactam family antibiotic, amoxicillin (AMX), from the other drugs, penicillin and ampicillin, on multiwalled carbon nanotube modified glassy carbon electrodes (GCE/AMX@MWNT), without any linkers and surface functionalization, has been successfully demonstrated. The electrochemical response of the AMX on GCE/MWNT showed an irreversible oxidation peak at 0.5 V *vs.* Ag/AgCl (A1), followed by the growth of a new redox peak at 0 V *vs.* Ag/AgCl (A2/C2) in pH 7 phosphate buffer solution, which is in parallel to a control phenol electrochemical response, revealed that the phenoxy radical electrogenerated at A1 gets subsequently adsorbed on the underlying MWNT modified electrode with a specific surface confined A2/C2 redox peak with proton-coupled electron transfer behaviour. Physicochemical characterization from X-ray diffraction, transmission electron microscopy and scanning electron microscopy collectively evidenced the immobilization of AMX both on the inner and outer (surface) walls of the carbon nanotubes. Further, the AMX@MWNT hybrid material was found to show enhanced antibacterial activity against three bacterial pathogens, *Escherichia coli*, *Staphylococcus aureus* and *Bacillus subtilis*, over the unmodified AMX and MWNT. Finally, as an environmental pollution remedy, the uptake of the AMX drug from five different simulated sources: river water, sea water, river soil, sea soil and farm milk, was successfully demonstrated by this new electrochemical methodology.

Introduction

Hybrid nano-biomaterials composed of carbon nanotubes (CNTs) and therapeutic drugs have recently been of tremendous interest in nanomedicine, nanodrug delivery and nanobiotechnology applications.[1–6] Oxygen group functionalized and hydrophilic natured CNTs were considered to be biocompatible and supportive therapeutic candidates (*i.e.*, pharmaceutical excipients) for creating versatile drug delivery systems.[4,7–10] There are three types of interaction route *viz*, (i) adsorption/immobilization through a porous structure or π–π interactions, (ii) functional attachment and (iii) encapsulation, available for the hybrid CNT–pharmaceutical drug preparations. Amongst them, functional group interactions in which oxygen rich surface functional groups such as carboxylic acid, carbonyl and phenolic, generated on CNTs covalently attach to amine-terminated pharmaceutical drug solution phase, is considered to be a promising synthetic route.[4] For instance, functionalized single walled (SWNT*, * = functionalized) or mulltiwalled (MWNT*) carbon nanotubes are covalently attached to amphotericin B (AmB) through a biopolar amino linker for therapeutic use in transfection and for increased antifungal activity.[8] Meanwhile, a few π–π interaction based hybrid CNT–drug systems were also reported, with an example being the anticancer drug doxorubicin (DOX) with stacked SWNT*, where the DOX was adsorbed on the polyethylene glycol (which acts as a linker) functionalized SWNT* surface.[1,5] For the first time in the literature, we demonstrate the electrochemically assisted stable immobilization of a β-lactam structured penicillin antibiotic drug, amoxicillin (D-α-amino-p-hydroxy-benzylpencillin trihydrate, AMX) selectively on CNT modified glassy carbon electrodes (GCE) without any linkers, in a neutral pH 7 phosphate buffer solution (PBS).

Amoxicillin is a broad spectrum antibiotic which is used to treat respiratory, ENT (ear nose and throat), skin and soft tissue infections caused by certain organism such as *Escherichia coli* (*E. coli*), *Bacillus subtilis* (*Bacillus*) and *Staphylococcus aureus* (*S. aureus*) *etc.*[11,12] Apart from the therapeutic uses, large quantities of the AMX are also used as supplements that are provided illegally to promote growth in food-producing animals,[13] including for aquaculture and in cattle rearing. Formation of AMX residues in fish tissues and milk leads to serious health issues for human, and removal of the waste drug from water sources is a challenging environmental pollution problem.[14,15] There are some bulk materials used for the adsorption/immobilization of solution phase AMX which include chitosan beads,[16] activated carbon,[17] iron nanoparticles,[18] and functionalized

[a]*Environmental and Analytical Chemistry Division, School of Advanced Sciences, Vellore Institute of Technology University, Vellore, 632 014, India. E-mail: askumarchem@yahoo.com; Fax: +91 416 2243092; Tel: +91 -416- 2202754*
[b]*Division of Biomolecules and Genetics, School of Biosciences and Technology, Vellore Institute of Technology University, Vellore, 632 014, India*
[c]*Department of Chemistry, National Chung Hsing University, Taichung, 402, Taiwan*

† Electronic supplementary information (ESI) available: CV responses for the AMX@MWNT powder modified electrode (Figure S1), various amines functionalized organic molecules for the immobilization on the GCE/MWNT (Figure S2) and uptake of AMX from various simulated environmental samples (Figure S3). See DOI: 10.1039/c0jm02262d

sol–gel SiO_2[19] synthesised by surface functionalization mechanism. Other antibiotics *viz*, sulfonamide,[20] norfloxacin,[21] tetracycline[22,23] and sulfamethoxazole[23] were reported to adsorb onto CNTs by the solution phase methodology. In this work, we observed unusual, selective and stable electro-assisted immobilization of AMX on CNT modified GCE (designated as GCE/AMX@CNT) with a marked surface confined redox-peak without any functional linkers at 0 V *vs.* Ag/AgCl in pH 7 PBS. Also, other β-lactam penicillin antibiotic drugs such as penicillin (PENI) and ampicillin (AMPI) failed to show any such new redox peak response at lower potentials (Scheme 1A). The CNT–AMX hybrid material shows enhanced antimicrobial activity against *E. coli*, *S. aureus* and *Bacillus*, which is demonstrated for the first time here.

Experimental

Chemicals and reagents

Amoxicillin, multi-walled (MWNT) and single-walled (SWNT) carbon nanotubes were purchased from Sigma-Aldrich. Amoxicillin tablets were collected from local hospital. Other chemicals used were all of ACS-certified reagent grade and used without further purification. Screen-printed gold electrodes were purchased from Zensor R&D, Taiwan. Aqueous solutions were prepared using deionized and alkaline potassium permanganate ($KMnO_4$) distilled water (designated as DD water). Unless otherwise stated, pH 7 phosphate buffer solution (PBS) of ionic strength, $I = 0.1$ M was used as the supporting electrolyte.

Instrumentation

Voltammetric measurements were all carried out with a CHI Model 660C electrochemical workstation (USA). The three-electrode system consists of glassy carbon or screen-printed substrates and its chemically modified electrodes as the working electrode (0.0707 cm^2), Ag/AgCl as the reference electrode and platinum wire as the auxiliary electrode. High resolution transmission electron microscopy (TEM) was carried out using an EM902A, Zeiss operating at 80 kV, Field emission scanning electron microcopy (SEM) was done using a Carl Zeiss SMT, Ultra Plus Germany and X-ray diffraction (XRD) was performed using a Burker D8 Advanced system.

Procedures

Functionalized and purified multiwalled carbon nanotubes (MWNT* and MWNT^P) were prepared by treating the as received MWNT with concentrated (13 N HNO_3) and diluted (2 N HNO_3) acid solutions as per the literature.[24,25] MWNT, MWNT*, MWNT^P and SWNT modified GCEs (*i.e.*, GCE/CNTs) were prepared by the following procedure: 3 μL of the respective carbon nanotubes were dispersed in ethanol (2 mg/500 μL) and was drop coated on the cleaned GCE electrode (net amount of CNTs on the surface = 12 μg) and dried in air for 15 min at room temperature. Since dissolved oxygen does not influence the present electrochemical system, the experiments were all performed with normal dissolved oxygen.

For the GCE/AMX@MWNT preparation, 1 mM amoxicillin in pH 7 phosphate buffer solution was potential cycled with GCE/MWNT in the potential window −0.2 V to 0.7 V *vs.*

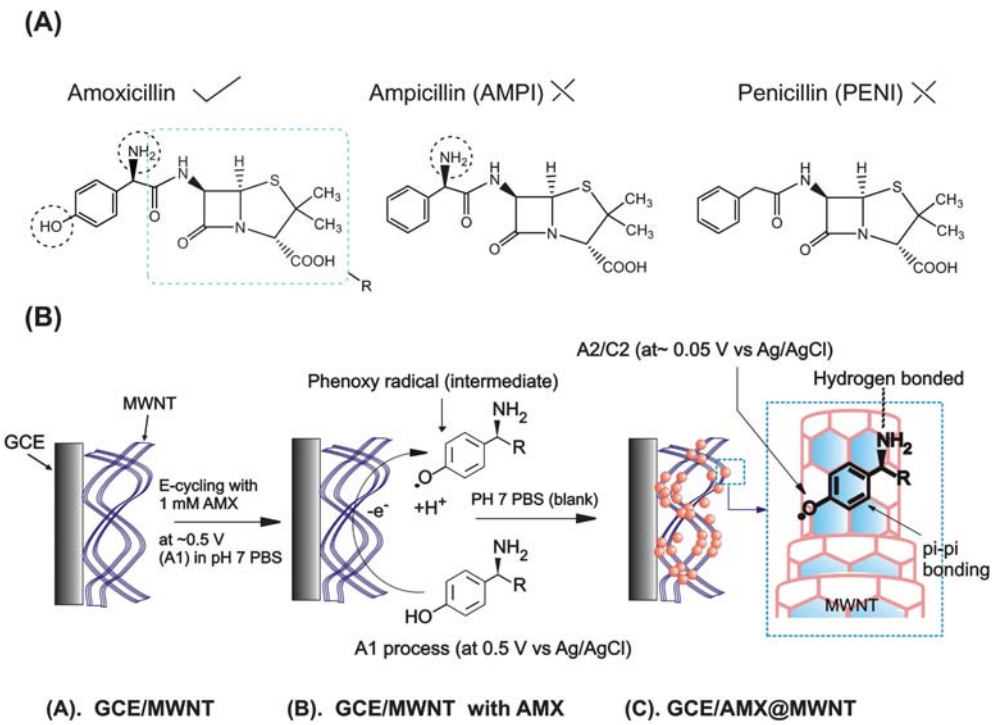

Scheme 1 (A) Comparative chemical structure of various β-lactam family antibiotics. (B) Cartoon for the electrochemical procedure for the immobilization of amoxicillin (AMX) on glassy carbon modified MWNT electrode and its AMX stabilized structure. Dotted circles in (A) indicate possible active groups.

Ag/AgCl at scan rate (v) = 50 mV s^{-1} for no. of cycles (n) = 20, followed by washing with copious amount of water and then moved to blank pH 7 PBS for the stabilization (n = 20) of the GCE/AMX@MWNT in a potential window of −0.2 V to 0.6 V *vs.* Ag/AgCl. Note that the CV responses of GCE/AMX@MWNT prepared from commercial tablet and Aldrich samples were quantitatively and qualitatively similar in their characteristics. Determination of amoxicillin surface coverage, Γ_{AMX} (nmol cm^{-2}) was obtained by integrating the anodic peak area (Q_a) of the cyclic voltammograms measured from the 10th cycle at v = 50 mV s^{-1}, and taking $\Gamma_{AMX} = Q_a/nFA$, where the number of electrons (n) = 1 and A is the geometrical surface area.

For practical convenience physicochemical characterization by SEM was carried out with gold screen-printed underlying electrode (*i.e.*, AuSPE/AMX@MWNT) prepared by the same electrochemical preparation procedure as above, which also shows qualitatively similar electrochemical patterns to that of the GCE/AMX@MWNT (data not shown). For the XRD, TEM and antibacterial experiments, simulated AMX@MWNT samples were prepared by solution phase procedure as follows: 10 mg MWNT and 5 mg amoxicillin were dissolved in pH 7 PBS and continuously stirred for 30 min at room temperature, DD water washed more than five times to completely remove the loosely adsorbed AMX (until the washings gave a negative signal to AMX) and dried in vacuum overnight. In order to check the active site present in the AMX@MWNT powder, 2 mg of the sample was dispersed in 500 μL of ethanol, drop coated on cleaned GCE and CV cycled as given in ESI Figure S1†. The powder sample showed qualitatively similar A2/C2 CV pattern with that of the GCE/AMX@MWNT with a Γ_{AMX} value of 0.6 nmol cm^{-2} (*ca.* 35.26 μg/800 μg of MWNT), which is about 6 times lower than that of electrochemically prepared sample value of 3.8 nmol cm^{-2}. Wet air oxidation of phenol is expected to occur in the solution phase procedure, which in turn became stabilized within the MWNT.[26]

Antibacterial activity

Antibacterial activity of amoxicillin against *Escherichia coli* (ATCC 25922), *Staphylococcus aureus* (ATCC 25923) and *Bacillus subtilis* (MTCC 2063) were tested using the well-diffusion method following the standard Kirby–Bauer method adopted by the National Committee for the Clinical Laboratory Standards.[27,28] The nutrient agar (28 g/1000 mL DD water) prepared was sterilized and poured in sterile petriplates and allowed to solidify. Overnight bacterial culture was raised in the nutrient broth (30 g/100 mL) from which a lawn culture of the test organism was made on the surface of the nutrient agar. The growth of the organism is seen as the confluent growth on the agar surface. Wells were cut using a sterile well borer on the agar surface seeded with test organisms. 200 μL of the samples (800 μg each of MWNT, drug and drug@MWNT (calculated net AMX site = 35.26 μg) dispersed in pH 7 PBS and washed) were added into each well and the discs of amoxicillin, ampicillin and penicillin (10 μg each) were used as standards. The plates were incubated at 37 °C overnight and examined for the zone of inhibition.[24] The zone of inhibition value is the diameter of the zone found around the well which determines the magnitude of the activity. The higher the zone size, higher is the activity against the bacteria.

Environmental sample analysis

Five real samples *viz*, river water, sea water, river soil, sea soil and farm milk, were taken as source to prepare simulated real samples. 5 mg of the soil samples were digested by using pH 7 PBS, prior to analysis. Filtered and four times diluted samples were pH adjusted to pH 7 using PBS, this was taken as the standard conditions for the experiment. Simulated AMX real samples were prepared by adding 1 mM of AMX directly to 10 mL of the real samples. Electro-chemical uptake of AMX from the real samples was carried out in a similar way to GCE/AMX@MWNT preparation (Fig. 1A), except with 1 mM AMX added to 10 mL pH 7 PBS preparation bath.

Results and discussion

Electrochemical assisted immobilization of AMX on MWNT

The CV response of 1 mM of AMX on GCE/MWNT in the potential window −0.5–0.7 V *vs.* Ag/AgCl at a v = 50 mV s^{-1} is displayed in Fig. 1A. The first anodic forward scan shows an irreversible anodic peak at 0.5 V (A1) and a feeble appearance of its counter peak at 0.05 V (C2) in the reverse cathodic cycle, and the 2nd forward scan yields a corresponding anodic counter peak at 0.06 V (A2). The A2/C2 redox peak current behavior started to grow systematically upon continuous cycling along with a decreased current response at 0.5 V on the anodic side. Additionally, a control CV measurement in the potential window −0.2–0.4 V for the preparation of GCE/AMX@MWNT didn't not show redox behavior at 0 V *vs.* Ag/AgCl (Fig. 1(A)b), which attributes the necessity of the pre-oxidation condition at >0.5 V to the appearance of the new A2/C2 redox behavior. Meanwhile, an unmodified GCE was also subjected to the immobilization process as in Fig. 1(A)b experiment, but failed to show any redox response in the entire potential window (data not shown). After the AMX experiment (Fig. 1(A)a), the GCE/MWNT working electrode was washed and the medium replaced with blank pH 7 PBS and the CV cycled 20 times (n = 20), shown in Fig. 1(B)a. Interestingly a stable redox peak response with peak-to-peak separation ($\Delta E_p = E_{pa} - E_{pc}$), surface excess ($\Gamma_{AMX}$) and formal electrode potential ($E^{o\prime}$) values of 20 mV, 3.8 nmol cm^{-2} (*ca.* 0.76 wt%) and 50 mV *vs.* Ag/AgCl respectively was achieved. Twenty continuous CV measurements (n = 20) yielded a relative standard deviation (RSD) of 1.9% for the A2 peak, suggesting that the electrochemical behavior of the A2/C2 redox peak is stable. In connection to the experiment, other β-lactam penicillin antibiotic drugs; penicillin and ampicillin, were also subjected to the immobilization studies on GCE/MWNT (Fig. 1(C)). Interestingly, the absence of any redox peak response at 0 V, was noticed with theses compounds, revealing the selective immobilization of AMX on the GCE/MWNT electrode. The presence of the phenolic (Ph–OH) functional group in AMX is a specific reason for its selective immobilization. Initially, we expected that the impurities (metal and amorphous carbon) and the functional groups (carbonyl, alcoholic carboxylic and ether) present in the MWNT to be the responsible candidates for AMX's electro-assisted immobilization on GCE/MWNT

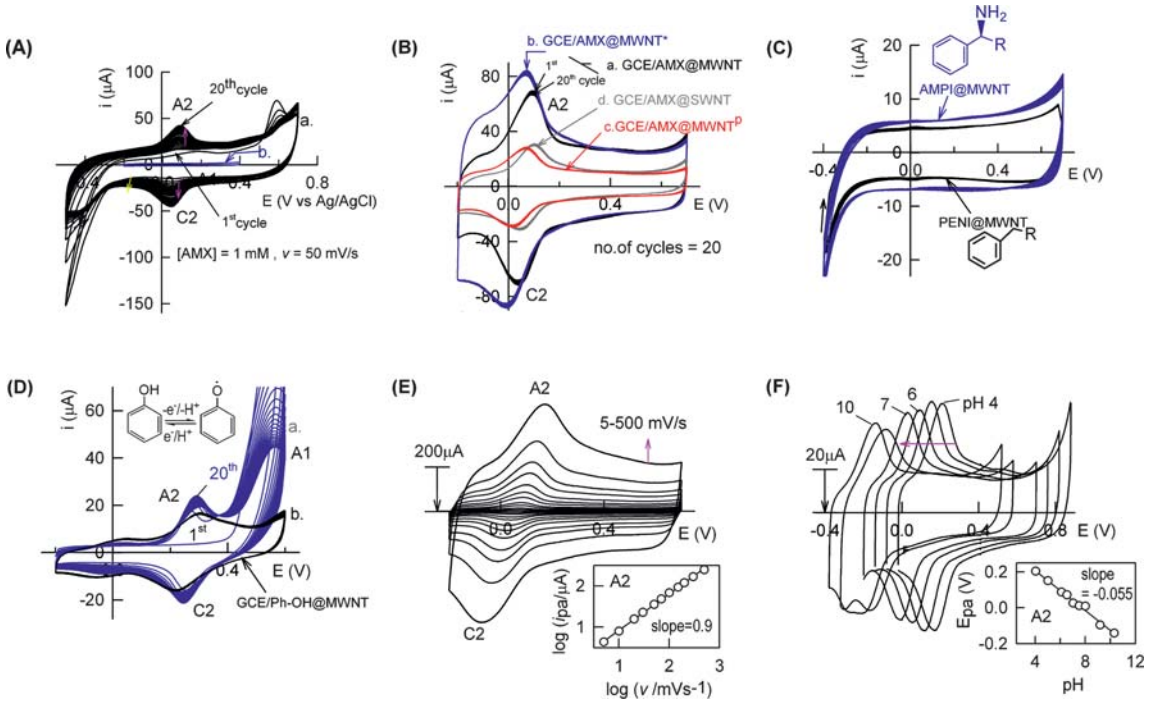

Fig. 1 Twenty continuous CV responses of (A) GCE/MWNT with 1 mM of amoxicillin (AMX) at different potential windows (a, b), (B) various AMX electrochemically adsorbed CNT modified electrodes (a–d), (C) penicillin (PENI) curve (a) and ampicillin (AMPI) curve (b) electrochemically adsorbed onto GCE/MWNT and (D) GCE/MWNT with 1 mM of phenol (curve a) and the electrochemically adsorbed GCE/Ph@MWNT (curve b) in pH 7 PBS at a scan rate (v) of 50 mV s^{-1}. CV of GCE/AMX@MWNT (E) with increasing scan rates in pH 7 PBS and its double logarithmic plot of i_{pa} *vs.* v (inset) and (E) with different pHs (4–10) at a scan rate of 50 mV s^{-1} and its E_{pa} *vs.* pH plot (inset).

(i.e, GCE/AMX@MWNT). Control CV experiments as in Fig. 1(B)b–d with various CNTs; MWNT*, purified MWNT ($MWNT^P$) and SWNT modified GCE showed similar redox patterns with an $E^{o\prime}$ value of ~50 mV *vs.* Ag/AgCl, this excludes specific qualitative effects from impurities present in the MWNT. However, an ~20% quantitative increase in the A2-i_{pa} response with the GCE/AMX@MWNT* (RSD = 4.9%) attributes a partial contribution to the open ended surface functional group and edge plane effect (open ended structure with large surface holes) as proposed by the Compton group,[29] that are responsible for the relatively large amount of intake of antibiotics seen here. On the other hand, the relatively lower amoxicillin intake for the $MWNT^P$ compared to the MWNT might be due to the metal (Fe, Ni *etc*) impurities present in the "as received MWNT" which may contribute the immobilization through some complexation mechanism which is unknown to us right now. On the whole, the presence of impurities is an added advantage to enhance the accumulation of antibiotics within the CNT matrix. Due to a lower RSD value observed for the GCE/AMX@MWNT (Fig. 1(B)a), this material is used for further electrochemical analysis.

Mechanism for the AMX immobilization

The phenolic sites of the AMX (ϕ–Ph–OH) and its electro-oxidized species at 0.5 V (A1) are the key factors for the immobilization process. Mathiyarasu *et al.* observed highly irreversible oxidation of phenol to the phenoxy radical at 0.55 V *vs.* Ag/AgCl on GCE with pH 7 PBS.[30] It has been reported that the phenoxy radical undergo a spontaneous polymerization reaction on the underlying electrode surface which in turn leads to the deactivation of the working electrode.[30,31] On the other hand, Wang and Dea observed a phenol electrochemical oxidation without any deactivation step at 0.5 V *vs.* Ag/AgCl on Nafion/CNT chemically modified electrode and suggested that there was no polymerization of the phenoxy intermediate in their work.[32] In connection to these reports, a control CV experiment with 1 mM of phenol on GCE/MWNT was carried out as in Fig. 1(D)a, where an irreversible oxidation peak at 0.5 V (A1) was followed by growth of a highly reversible redox peak at 0.3 V *vs.* Ag/AgCl (A2/C2) was observed, which is closer to the case for the GCE/AMX@MWNT in Fig. 1(A)a. After continuous potential cycling with phenol solution, the electrode was washed and the medium replaced with blank pH 7 PBS. The A2/C2 peak was still retained on the surface (*i.e.*, GCE/Ph-OH@MWNT) with formal potential and peak current RSD values of 0.27 V and 3.6% respectively (Fig. 1(D)b). This observation confirms the phenolic site contribution for the A2/C2 peak with GCE/AMX@MWNT. An ~0.22 V positive shift in the A2/C2 redox peak of the bare phenol (Fig. 1(D)a) compared to the AMX (Fig. 1(A)a), is due to the additional chemical structures. Meanwhile, the possibility for the involvement of AMX's amino functional group in the electron-transfer behaviour of GCE/AMX@MWNT was ruled out, since control experiments for the immobilization of ampicillin and other simple amino organic compounds (ethylamine, ethanolamine and benzyl amine, ESI Figure S2†) on GCE/MWNT, failed to show any electron-transfer signals even in the wide potential window of −0.6–0.9 V *vs.* Ag/AgCl. Note that the

electrochemical grafting of amines on carbon surfaces, were reported only at high operation potential of >1.2 V *vs.* Ag/AgCl in ~pH 4–7.[33] Scheme 1 provides a possible mechanism for the immobilization and electron-transfer behaviour of AMX@MWNT. On the whole, the electrochemically generated phenoxy radical gets stabilized within the walls of CNTs through π–π bonding between the AMX's aromatic electrons and sp^2 carbon on the CNT, particularly in the strained and misaligned areas of the CNT,[34,35] is a possible mechanism for the selective immobilization process.

Electrochemical characterization

The CV scan rate (v) effect on GCE/AMX@MWNT shows a systematic increase in the peak current response upon increasing the scan rate (v) in the window of 5–500 mV s^{-1} (Fig. 1(E)). A double logarithmic plot of the anodic peak current, i_{pa} *vs.* v yielded a slope ($\partial \log i_{pa}/\partial \log v$) of 0.9 (inset Fig. 1(E)), close to an ideal value of 1, indicates a surface confined electron-transfer mechanism for the A2/C2 redox process.[35] The effect of pH on the CV response of GCE/AMX@MWNT shows a negative potential shift in the CV response (Fig. 1(F)) and a plot of anodic peak potential, E_{pa} *versus* pH resulted in a slope of value ($\partial E_{pa}/\partial pH$) = −0.055 V/decade (inset Fig.1(F)), which is closer to the ideal Nernstian value of −0.059 V/decade. This corresponds to an equal amount of e^-/H^+ involvement as proposed for the electrochemical reaction: ϕ–Ph–OH ⇔ ϕ–Ph–O. + $H^+ + e^-$ in this work, unlike the previously reported value of −0.045 V/decade with the non-Nernstian condition for the AMX oxidation process at 0.6 V *vs.* Ag/AgCl (A1) on the GCE/Nafion–MWNT.[31] Further physicochemical characterizations by XRD, TEM and SEM support the stabilization of the AMX active sites within the CNT.

Physicochemical characterization

Fig. 2 is a comparative XRD analysis of AMX, MWNT and AMX@MWNT. Unmodified AMX and MWNT samples show distinct and intense 2θ peaks, attributed to the crystalline behaviour of the respective materials. Interestingly, the XRD pattern of AMX@MWNT displayed in Fig. 2C is similar to that of MWNT with additional low angle 2θ peaks at 21.5° and 25.5° and high angle peaks at 30.7° and 38.1°, with respect to MWNT's major peak at 26.27°. Based on our recent published report on a catechol encapsulated MWNT system with a peak at 12.15°,[35] we propose that the lower and higher 2θ peaks are due to the inner multi-walls encapsulated (π–π bonded) and outer surface adsorbed AMX species respectively. In order to further confirm the observation, TEM and SEM experiments were carried out with the AMX@MWNT samples, as in Fig. 3A/B and C respectively. Fine black spots within the walls of the MWNTs were clearly seen in the AMX@MWNT samples (designated as $\{AMX@MWNT\}_{walls}$, Fig. 3A and B), while bigger spots with an area larger than the wall diameters due to the surface adsorbed AMX on the MWNT (designated as $\{AMX@MWNT\}_{surf}$) were observed in the TEM images. Parallel SEM analysis using the same sample also display the different kinds of AMX immobilization (Fig. 3C). For comparison, an electroinactive antibiotic, ampicillin was also subjected to TEM and SEM as

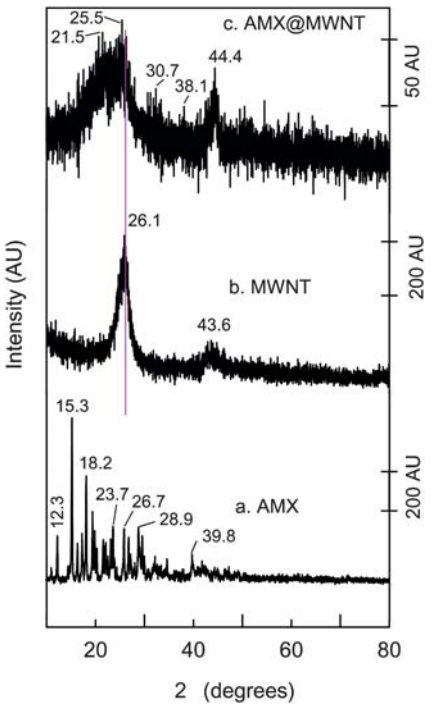

Fig. 2 XRD patterns of different powder samples.

shown in Fig. 3D/E and F respectively. Except for few impurity spots, there is no sign of the inner wall adsorbed drug species in the TEM, while white spot of diameter ~200 nm were identified in the SEM due to the surface adsorbed species, this further supports the mechanism proposed in Scheme 1 for the selective immobilization of AMX within the MWNT.

Antibacterial studies

Antibacterial activity for the AMX@MWNT powder sample (active site concentration *ca.* 35.26 μg/800 μg of MWNT) against *E. coli* (gram negative organism) were investigated next by measuring the zone of inhibition,[36] in comparison to the respective unmodified samples; AMX (800 μg) and MWNT (800 μg) were dissolved and suspended in 200 μL of pH 7 PBS. Increase in the zone diameter indicates increase in the antibacterial activity. As can be seen in Fig. 4A, the action of a commercial AMX disc (A), AMX drug solution (I), MWNT (II) and AMX@MWNT (III) powder suspensions against *E. coli* bacteria yielded respective zone of inhibition values of 1.5, 3.5, 0 (no zone) and 4.0 cm. The calculated relative % with respect to III, are 38, 88, 0 and 100% for A, I, II and III respectively. The 0% value with MWNT indicates the absence of any antibacterial activity in its unmodified state. It is interesting to notice that the active site concentration of the hybrid AMX@MWNT sample (35.26 μg) is 23 times lower than the same weight of AMX (800 μg), yet yields a 12% enhancement in activity. Similar comparative studies with AMPI@MWNT (Fig. 4B) and PEN-I@MWNT (Fig. 4C) powder samples show respective relative zone of inhibition values of 38, 100, 0 and 88%, (A, I, II and III for both the samples, % with respect to the drug), and were lower in the activity of the drug@MWNT hybrid units. This result is comparable to the case where absence of electrochemical activity

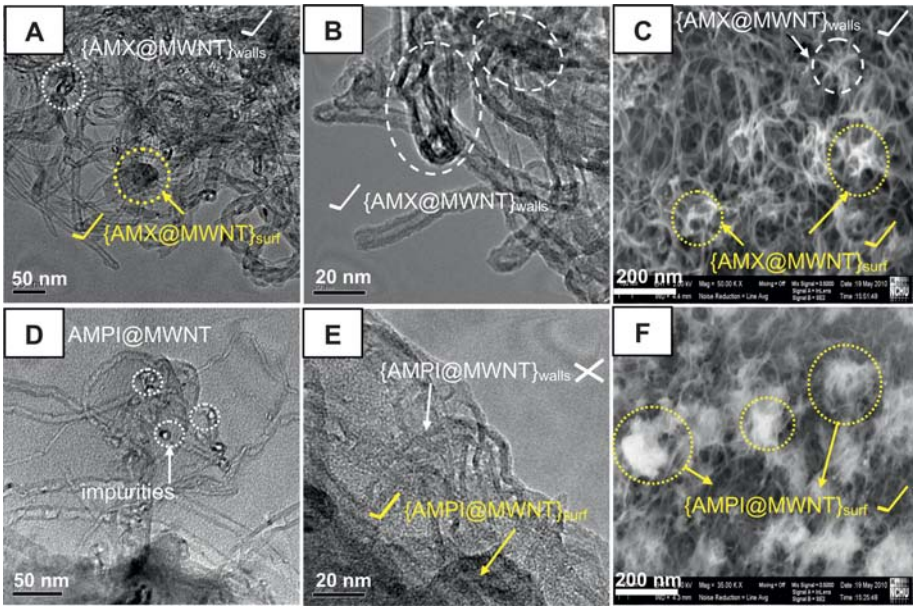

Fig. 3 TEM (A,B,D and E) and SEM (C and F) picture of AMX@MWNT (A–C) and AMPI@MWNT (D–F) samples.

with the drugs was observed, as in the Fig. 1C. Extended antibacterial activities of the AMX@MWNT towards other gram positive organisms: *Staphylococcus aureus* and *Bacillus subtilis*, also yielded similar enhancement in the activity over the unmodified AMX and MWNTs (Table 1). The absence of any antibacterial activity towards the AMX-disc, might be due to the lower concentration (10 μg) used in the control sample. On the whole, the marked enhancement in the antibacterial activity of AMX@MWNT over the PENI and AMPI modified MWNT, seen here is new and unusual. Possibly, the MWNT stabilized phenoxy radical (Fig. 1A and B), is an additional factor for the enhanced antibacterial activity of the CNT–drug hybrid material. This is also the reason why relatively lower antibacterial activity is seen for the other hybrid CNT–drug materials, PENI@MWNT and AMPI@MWNT. Note that another *in vitro* method suitable for studying antibacterial activity is the "Minimum Inhibitory Concentration" method.[37] In this approach the difference in the UV-Vis absorption of the organism + drug and organism in a serial dilution, is taken as a measure of antibacterial activity. Unfortunately, such a methodology is not suitable for solid or heterogeneous samples, like CNT@AMX, since it is highly difficult to analyse the activity using UV-Vis.

Environmental pollution remedy

The proposed electrochemical method was tested for the uptake of amoxicillin found in drug contaminated milk, water and soil samples. Accordingly, five simulated real samples were prepared *viz.* river water, sea water, river soil, sea soil and farm milk and subjected to the electrochemical uptaking method as given in the ESI Fig. S3A–E†. The concentration (Γ_{AMX}) of AMX loaded on MWNT modified GCE was calculated as 0.52, 1.4, 0.76, 0.79, 0 and 0.1 nmol cm^{-2} and the respective weight% values are 0.1, 0.3, 0.2, 0.2 and 0.02, clearly proving the uptake of the AMX by this new electrochemical methodology. Additionally, this method can be extended to real time applications like amoxicillin contaminated waste water recycling processes, in which AMX

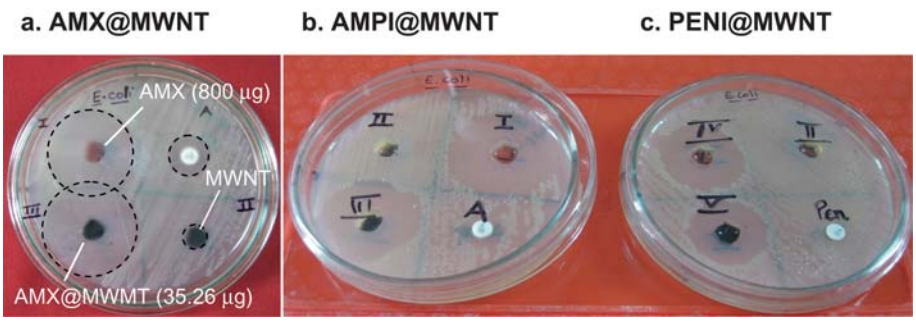

Fig. 4 Antibacterial activity for AMX@MWNT (a), AMPI@MWNT (b) and PENI@MWNT (c) hybrid systems against *E. coli*. Symbols A (a, b) and Pen (c) indicate the respective standard pharmaceutical drug disc; I (a, b) or IV (c) = unmodified drug (800 μg in 200 μL solution); II = unmodified MWNT (800 μg in 200 μL dispersion) and III (a, b) or V (c) = drug@MWNT hybrid sample (800 μg in 200 μL dispersion). For AMX@MWNT, [AMX] = 35.26 μg.

Table 1 Results of the comparative antibacterial activity for AMX@MWNT, MWNT and AMX

	Zone of inhibition value in cm (relative %)			
Organism	*Control[c]	*AMX[d]	*MWNT[e]	*AMX@MWNT[f]
[a]*E. coli*	1.5 (38)	3.5 (88)	No zone	4.0 (100)
[b]*S. aureus*	—	2.0 (87)	No zone	2.3 (100)
[b]*Bacillus*	—	1.5 (75)	No zone	2.0 (100)

[a] gram negative organism. [b] gram positive organism. [c] Control =10 μg amoxicillin disc. [d] [AMX] = 800 μg (in 200 μL). [e] MWNT = 800 μg (in 200 μL). [f] [AMX]@MWNT = 35.26 μg (in 200 μL).

pollutant uptake using a MWNT system (possibly in the form of a MWNT packed column) can be achieved from an environmental sample (like water from a fish tank used in aquaculture or from the feed stock of milk producing animals) and can be subsequently used for its antibacterial activity.

Conclusions

In conclusion, a new electrochemical way to highly selectively immobilize the β-lactam antibiotic amoxicillin (AMX) from the other drugs of same group (penicillin and ampicillin) within the carbon nanotube of a modified electrode, was successfully demonstrated. The phenolic site present in AMX is found to be selectively involved in the stabilization process. During the electrochemical oxidation of the AMX on MWNT modified GCE (GCE/MWNT), an irreversible peak at 0.5 V *vs.* Ag/AgCl (A1) is seen, and is due to the generation of a phenoxy intermediate radical, which is subsequently stabilized within the MWNT interface through a π–π interaction, the resulting species was observed with a specific stable redox peak at 0.05 V *vs.* Ag/AgCl (A2/C2). Control electrochemical experiments with penicillin and ampicillin drugs of the β-lactam antibiotic family, failed to show any such new redox peak appearance. Physicochemical characterization of AMX@MWNT in comparison with unmodified systems by XRD, TEM and SEM, collectively suggested that both the presence of both inner walls and outer surface adsorbed AMX species. TEM and SEM pictures of the hybrid sample specifically support these observations. Extended antibacterial activity of the AMX@MWNT system showed an enhanced response over the unmodified AMX and MWNT. Specific phenoxy radical participation within the MWNT matrix was the additional source of the enhanced activity. Finally, an electrochemical procedure for the uptake of AMX from five different simulated real samples, was successfully demonstrated as a remedy to the environmental AMX drug pollution problem.

Acknowledgements

The authors thank the financial support from the Department of Science and Technology (DST), India. We also thank Professor K. Kannabiran for his help in carrying out the antibacterial studies. This work is partially supported from the Indo-Taiwan joint project from the Confederation of Indian Industry, India and National Science council of China, Taiwan.

References and notes

1 Z. Liu, X. Sun, N. Nakayama-Ratchford and H. Dai, *ACS Nano*, 2007, **1**, 50–56.
2 S. J. Son, X. Bai and S. B. Lee, *Drug Discovery Today*, 2007, **12**, 650–656.
3 M. Foldvari and M. Bagonluri, *Nanomed.: Nanotechnol., Biol. Med.*, 2008, **4**, 173–182.
4 M. Foldvari and M. Bagonluri, *Nanomed.: Nanotechnol., Biol. Med.*, 2008, **4**, 183–200.
5 Z. Liu, A. C. Fan, K. Rakhra, S. Sherlock, A. Goodwin, X. Chen, Q. Yang, D. Felsher and H. Dai, *Angew. Chem., Int. Ed.*, 2009, **48**, 7668–7672.
6 F. Lu, L. Gu, M. J. Meziani, X. Wang, P. G. Luo, L. M. Veca, L. Cao and Y.-P. Sun, *Adv. Mater.*, 2009, **21**, 139–152.
7 K. Kostarelos, *Nat. Biotechnol.*, 2008, **26**, 774–776.
8 W. Wu, S. Wieckowski, G. Pastorin, M. Benincasa, C. Klumpp, J.-P. Briand, R. Gennaro, M. Prato and A. Bianco, *Angew. Chem., Int. Ed.*, 2005, **44**, 6358–6362.
9 S. Nagarajan, T. Mohan Das, P. Arjun and N. Raaman, *J. Mater. Chem.*, 2009, **19**, 4587–4596.
10 S. Nagarajan and T. Mohan Das, *New J. Chem.*, 2009, **33**, 2391–2396.
11 J.-M. Pagès, C. E. James and M. Winterhalter, *Nat. Rev. Microbiol.*, 2008, **6**, 893–903.
12 C. Ponte, M. Gracia, M.-J. Giménez and L. Aguilar, *Clin. Ther.*, 2005, **27**, 1043–1049.
13 L. Kantiani, M. Farre', M. Sibum, C. Postigo, M. Lo' pez de Alda and D. Barcelo', *Anal. Chem.*, 2009, **81**, 4285–4295.
14 R. Andreozzi, V. Caprio, C. Ciniglia, M. D. Champdorea, R. L. Giudice, R. Marotta and E. Zuccato, *Environ. Sci. Technol.*, 2004, **38**, 6832–6838.
15 C. Y. W. Ang, F. F. Liu, O. Jack Lay, Jr., W. Luo, K. McKim, T. Gehring and R. Lochmann, *J. Agric. Food Chem.*, 2000, **48**, 1673–1677.
16 W. S. Adriano, V. Veredas, C. C. Santana and L. R. B. Goncalves, *Biochem. Eng. J.*, 2005, **27**, 132–137.
17 E. E. Putra, R. Pranowo, J. Sunarso, N. Indraswati and S. Ismadji, *Water Res.*, 2009, **43**, 2419–2430.
18 A. Ghauch, A. Tuqan and H. A. Assi, *Environ. Pollut.*, 2009, **157**, 1626–1635.
19 Z. Li, K. Su, B. Cheng and Y. Deng, *J. Colloid Interface Sci.*, 2010, **342**, 607–613.
20 L. Ji, W. Chen, S. Zheng, Z. Xu and D. Zhu, *Langmuir*, 2009, **25**, 11608–11613.
21 L. Ji, W. Chen, L. Duan and D. Zhu, *Environ. Sci. Technol.*, 2009, **43**, 2322–2327.
22 L. Ji, F. Liu, Z. Xu, S. Zheng and D. Zhu, *Environ. Sci. Technol.*, 2010, **44**, 3116–3122.
23 D. Zhang, B. Pan, H. Zhang, P. Ning and B. Xing, *Environ. Sci. Technol.*, 2010, **44**, 3806–3811.
24 P. D. Tam, *J. Immunol. Methods*, 2009, **350**, 118–124.
25 E. B. Craig, C. Alison, S. Christopher, J. W. Shelley and R. G. Compton, *Angew. Chem., Int. Ed.*, 2006, **45**, 2533–2537.
26 S. Yang, W. Zhu, X. Li, J. Wang and Y. Zhou, *Catal. Commun.*, 2007, **8**, 2059–2063.
27 National Committee for Clinical Laboratory Standards, *Performance standards for antimicrobial disc susceptibility tests*, Villanova, Pa, 1975.
28 A. Piozzi, I. Francolini, L. Occhiaperti, M. Venditti and W. Marconi, *Int. J. Pharm.*, 2004, **280**, 173–183.
29 A. F. Holloway, G. G. Wildgoose, R. G. Compton, L. Shao and M. L. H. Green, *J. Solid State Electrochem.*, 2008, **12**, 1337–1348.
30 J. Mathiyarasu, J. Joseph, K. L. N. Phani and V. Yegnaraman, *Indian J. Chem. Tech.*, 2004, **11**, 797–803.
31 L. Bao, R. Xiong and G. Wei, *Electrochim. Acta*, 2010, **55**, 4030–4038.
32 J. Wang and R. P. Dea, *Electroanalysis*, 2003, **15**, 23–24.
33 R. S. Deinhammer, M. Ho, J. W. Anderegg and D. Porter, *Langmuir*, 1994, **10**, 1306–1313.
34 X. Peng and S. S. Wong, *Adv. Mater.*, 2009, **21**, 625–642.
35 A. S. Kumar and P. Swetha, *Langmuir*, 2010, **26**, 6874–6877.
36 R. Ananthanarayan and C. K. J. Paniker, in *Textbook of Microbiology*, ed. C. K. J. Paniker, Orient Longman, India, 6th edn, 2000, part. V, ch. 66, pp. 581–583.
37 X.-F. Li, X.-Q. Feng, S. Yang, G.-G. Fu, T.-P. Wang and Z.-X. Su, *Carbohydr. Polym.*, 2010, **79**, 493–499.

